

## Durham Research Online

---

### Deposited in DRO:

24 April 2017

### Version of attached file:

Accepted Version

### Peer-review status of attached file:

Peer-reviewed

### Citation for published item:

Katus, T. and Grubert, A. and Eimer, M. (2015) 'Electrophysiological evidence for a sensory recruitment model of somatosensory working memory.', *Cerebral cortex.*, 25 (12). pp. 4697-4703.

### Further information on publisher's website:

<https://doi.org/10.1093/cercor/bhu153>

### Publisher's copyright statement:

This is a pre-copyedited, author-produced version of an article accepted for publication in *Cerebral cortex* following peer review. The version of record Katus, T. and Grubert, A. and Eimer, M. (2015) 'Electrophysiological evidence for a sensory recruitment model of somatosensory working memory.', *Cerebral cortex.*, 25(12): 4697-4703 is available online at: <https://doi.org/10.1093/cercor/bhu153>.

### Additional information:

## Use policy

---

The full-text may be used and/or reproduced, and given to third parties in any format or medium, without prior permission or charge, for personal research or study, educational, or not-for-profit purposes provided that:

- a full bibliographic reference is made to the original source
- a [link](#) is made to the metadata record in DRO
- the full-text is not changed in any way

The full-text must not be sold in any format or medium without the formal permission of the copyright holders.

Please consult the [full DRO policy](#) for further details.



**Electrophysiological evidence for a sensory recruitment model of somatosensory working memory**

Journal:	<i>Cerebral Cortex</i>
Manuscript ID:	CerCor-2014-00343.R2
Manuscript Type:	Original Articles
Date Submitted by the Author:	n/a
Complete List of Authors:	Katus, Tobias; Birkbeck College, Psychology Grubert, Anna; Birkbeck College, Psychology Eimer, Martin; Birkbeck College, Psychology
Keywords:	Electroencephalography (EEG), Selective Attention, Somatosensation, Working memory (WM), Event-related potentials (ERPs)

1  
2  
3 1 *Full Manuscript Title*

4  
5  
6 2 **Electrophysiological evidence for a sensory recruitment model of**  
7  
8 3 **somatosensory working memory**

9  
10  
11  
12 4  
13  
14 5 *Running Title*

15  
16  
17 6 **Sensory recruitment in tactile working memory**

18  
19  
20  
21 7  
22  
23 8 *Authors and Affiliations:* Tobias Katus<sup>a</sup>, Anna Grubert<sup>a</sup> & Martin Eimer<sup>a</sup>

24  
25  
26 9 <sup>a</sup>Department of Psychology, Birkbeck College, University of London, London  
27  
28 10 WC1E 7HX, United Kingdom.

29  
30  
31  
32 11  
33  
34 12 *Corresponding Author:* Tobias Katus

35  
36 13 Dept. of Psychological Sciences, Birkbeck College, University of London

37  
38 14 Malet Street, London WC1E 7HX

39  
40  
41 15 Phone: +44(0)20 7631 6522, Email: [t.katus@bbk.ac.uk](mailto:t.katus@bbk.ac.uk)

42  
43  
44  
45 16  
46  
47 17  
48  
49  
50 18  
51  
52 19 *Conflict of Interest:* The authors declare no competing financial interests.

53  
54  
55 20

56  
57  
58 21  
59  
60

1  
2  
3 22  
4  
56 **Abstract**  
7

8 24 Sensory recruitment models of working memory assume that information  
9 25 storage is mediated by the same cortical areas that are responsible for the perceptual  
10 26 processing of sensory signals. To test this assumption, we measured somatosensory  
11 27 event-related brain potentials (ERPs) during a tactile delayed match-to-sample task.  
12 28 Participants memorized a tactile sample set at one task-relevant hand to compare it  
13 29 with a subsequent test set on the same hand. During the retention period, a  
14 30 sustained negativity (tactile contralateral delay activity, tCDA) was elicited over  
15 31 primary somatosensory cortex contralateral to the relevant hand. The amplitude of  
16 32 this component increased with memory load and was sensitive to individual  
17 33 limitations in memory capacity, suggesting that the tCDA reflects the maintenance of  
18 34 tactile information in somatosensory working memory. The tCDA was preceded by a  
19 35 transient negativity (N2cc component) with a similar contralateral scalp distribution,  
20 36 which is likely to reflect selection of task-relevant tactile stimuli at the encoding stage.  
21 37 The temporal sequence of N2cc and tCDA components mirrors previous  
22 38 observations from ERP studies of working memory in vision. The finding that the  
23 39 sustained somatosensory delay period activity varies as a function of memory load  
24 40 supports a sensory recruitment model for spatial working memory in touch.

41  
42

43

44 **Introduction**  
45

46 44 Working memory (WM) is responsible for the active maintenance of  
47 45 information that is no longer perceptually present. Visual and tactile working memory  
48 46 are both assumed to be based on distributed neural networks that include prefrontal

49  
50  
51  
52  
53  
54  
55  
56  
57  
58  
59  
60

1  
2  
3 47 cortex (PFC) and modality-specific perceptual areas. The activation of PFC during  
4  
5 48 the maintenance of visual and tactile stimuli in working memory is well established  
6  
7 49 (Curtis and D'Esposito 2003; Curtis, Rao, D'Esposito 2004; Fuster and Alexander  
8  
9 50 1971; Kostopoulos, Albanese, Petrides 2007; Romo and Salinas 2003; Postle 2005).  
10  
11 51 Additionally, modality-specific visual (Harrison and Tong 2009; Supèr, Spekreijse,  
12  
13 52 Lamme 2001) or somatosensory areas (e.g., Kaas et al. 2013; Zhou and Fuster  
14  
15 53 1996) show persistent activation during the retention of visual or tactile stimuli.  
16  
17 54 Although the exact role of this delay-period activity in visual areas during working  
18  
19 55 memory maintenance and their link to selective visual attention are still debated (e.g.,  
20  
21 56 van Dijk et al. 2010; Lewis-Peacock et al. 2012; Postle et al. 2013), its existence has  
22  
23 57 led to the "sensory recruitment" model of working memory (D'Esposito 2007; Harrison  
24  
25 58 and Tong 2009; Pasternak and Greenlee 2005; Postle 2006). This model postulates  
26  
27 59 that perceptual brain regions which are responsible for the sensory processing of  
28  
29 60 visual or tactile stimuli are also involved in working memory storage. The sustained  
30  
31 61 activation of perceptual areas might be particularly important when working memory  
32  
33 62 tasks require the maintenance of detailed sensory information (e.g., Lee, Kravitz,  
34  
35 63 Baker 2013; see also Sreenivasan, Curtis, D'Esposito 2014).

36  
37 64 Support for the sensory recruitment model comes from ERP studies of visual  
38  
39 65 working memory (e.g., Vogel, McCollough, Machizawa 2005; Vogel and Machizawa  
40  
41 66 2004). In these studies, bilateral sample displays were followed after a retention  
42  
43 67 interval by test displays, and participants had to match sample and test objects on  
44  
45 68 one side of these displays. A sustained negativity at posterior electrodes contralateral  
46  
47 69 to the side of the memorized objects (contralateral delay activity, CDA) started 300  
48  
49 70 ms after sample onset and persisted throughout the retention interval. The fact that  
50  
51 71 this CDA component is sensitive to manipulations of visual working memory load and  
52  
53 72 to individual differences in working memory capacity strongly suggests that the CDA  
54  
55  
56  
57  
58  
59  
60

1  
2  
3 73 directly reflects the maintenance of visual information in working memory. The  
4  
5 74 contralateral nature and posterior scalp topography of the CDA is consistent with  
6  
7 75 neural generators in extrastriate visual areas (McCollough, Machizawa, Vogel 2007),  
8  
9  
10 76 in line with the sensory recruitment model. The CDA is typically preceded by an N2pc  
11  
12 77 component that emerges around 200 ms post-stimulus, has a similar posterior scalp  
13  
14 78 topography (e.g. McCollough, Machizawa, Vogel 2007), and reflects the attentional  
15  
16 79 selection and encoding of task-relevant objects in ventral visual cortex (Eimer 1996;  
17  
18 80 Luck and Hillyard 1994).

20  
21 81 While ERP markers of visual working memory are well established,  
22  
23 82 corresponding electrophysiological correlates of tactile working memory have not yet  
24  
25 83 been described. Here, we demonstrate the existence of two somatosensory ERP  
26  
27 84 components that are elicited during the encoding and maintenance of tactile stimuli in  
28  
29 85 working memory, and both show modality-specific topographies over primary  
30  
31 86 somatosensory cortex. We employed a task that was modelled on the delayed  
32  
33 87 match-to-sample task used in earlier studies of visual working memory (e.g., Vogel,  
34  
35 88 McCollough, Machizawa 2005; Vogel and Machizawa 2004). On each trial, a set of  
36  
37 89 tactile sample stimuli was followed after a 2000 ms retention period by tactile test  
38  
39 90 stimuli. Sample and test stimuli were delivered simultaneously to both hands, but the  
40  
41 91 memory task had to be performed for one of these hands only. Participants had to  
42  
43 92 encode and maintain tactile sample stimuli on the currently task-relevant hand, and to  
44  
45 93 match them to subsequent test stimuli on the same relevant hand. On low-load trials,  
46  
47 94 a single tactile stimulus had to be maintained and matched. On high-load trials, two  
48  
49 95 tactile pulses had to be memorized.

54  
55 96 Results revealed the existence of two somatosensory ERP components that  
56  
57 97 have not yet been described in the literature on tactile attention and working memory.  
58  
59 98 During the retention interval, a sustained tactile contralateral delay activity (tCDA)  
60

1  
2  
3 99 emerged with a modality-specific scalp distribution over somatosensory areas. This  
4  
5 100 tCDA component was sensitive to memory load and to individual differences in tactile  
6  
7 101 working memory capacity. It was preceded by a central contralateral negativity (N2cc  
8  
9 102 component) with a similar modality-specific topography that was also modulated by  
10  
11 103 working memory load. Analogous to the visual N2pc and CDA, these N2cc and tCDA  
12  
13 104 components reflect the spatially selective encoding and maintenance of task-relevant  
14  
15 105 information in tactile working memory.  
16  
17  
18  
19

106

## 107 **Materials and Methods**

### 108 **Participants**

109 Eighteen neurologically unimpaired paid adult participants were tested. The  
110 study was conducted in accordance with the Declaration of Helsinki, and was  
111 approved by the Psychology Ethics Committee, Birkbeck College. All participants  
112 gave informed written consent prior to testing. Two participants were excluded from  
113 analysis because their tactile WM capacity measured by Cowan's K (Cowan 2001)  
114 was below 1. Sixteen participants remained in the sample (mean age 32 years, range  
115 25-44 years, 3 male, 13 right-handed).  
116

116

### 117 **Stimuli and task design**

118 Participants were seated in a dimly lit recording chamber, viewing a monitor  
119 showing a central white fixation cross against a black background. Both hands were  
120 covered from sight and were placed on a table at a distance of approximately 40 cm.  
121 Eight mechanical tactile stimulators were attached to the distal phalanges of the  
122 index, middle, ring and small fingers of the left and right hand. Stimulators were  
123 driven by an eight-channel sound card (M-Audio, Delta 1010LT) and custom-built  
124 amplifiers, controlled by Matlab (MathWorks, Natick, MA). Continuous white noise  
125

60

1  
2  
3 125 was delivered via headphones to mask sounds produced by the tactile stimulators.

4  
5 126 All tactile stimuli were 100 Hz sinusoids (duration: 200 ms; intensity: 0.37 N).

6  
7 127 Figure 1 illustrates the experimental procedure. Each trial started with a set of

8  
9 128 tactile sample stimuli that were delivered simultaneously to the left and right hand.

10  
11 129 After a 2000 ms retention period, a set of tactile test stimuli was presented

12  
13 130 simultaneously to both hands. Prior to the start of each block, instructions displayed

14  
15 131 on the monitor informed participants whether the left or right hand was relevant in the

16  
17 132 upcoming block. Participants had to decide whether sample and test stimulus

18  
19 133 locations on this hand were identical (match trials) or different (mismatch trials). The

20  
21 134 task-relevant hand was swapped after each experimental block. Two load conditions

22  
23 135 were randomized within each block. In the *low-load condition*, one sample pulse was

24  
25 136 presented with equal probability to one of the four fingers of the left hand and the

26  
27 137 right hand. On match trials, the test pulse was delivered to the same finger of the

28  
29 138 relevant hand as the sample pulse. On mismatch trials, one of the three other fingers

30  
31 139 on that hand was stimulated at test. In the *high-load condition*, two sample pulses

32  
33 140 were presented to two randomly selected fingers of the left hand and the right hand,

34  
35 141 respectively. On match trials, test pulses were delivered to the same two fingers of

36  
37 142 the relevant hand. On mismatch trials, at least one of the two test pulses was

38  
39 143 presented to a different finger of that hand. Because one of the two sample locations

40  
41 144 could be repeated at test on mismatch trials, participants had to retain the location of

42  
43 145 both sample stimuli on the relevant hand to perform the task in the high-load

44  
45 146 condition. Match and mismatch trials were equiprobable. On the currently task-

46  
47 147 irrelevant hand, sample and test stimuli were also presented at matching or

48  
49 148 mismatching locations, and this was independent of whether there was a match or

50  
51 149 mismatch on the relevant hand.  
52  
53  
54  
55  
56  
57  
58  
59  
60



1  
2  
3 150 Participants signalled a match or mismatch between sample and test on the  
4  
5 151 relevant hand with a vocal response (“a” for match and “e” for mismatch) that was  
6  
7 152 recorded with a headset microphone between 200 ms and 1700 ms after test  
8  
9  
10 153 stimulus offset. A question mark replaced the fixation cross on the monitor during this  
11  
12 154 period. The interval between the offset of this question mark and the onset of the  
13  
14 155 sample pulses on the next trial varied between 800 and 1100 ms. The experiment  
15  
16 156 included ten blocks of 48 trials, with twelve trials per block for each of the four  
17  
18 157 combinations of high versus low load trials and match versus mismatch trials.  
19  
20  
21 158 Instructions emphasized accuracy over speed, and the need to avoid head and arm  
22  
23 159 movements and to maintain central gaze fixation. Feedback on hit and correct  
24  
25 160 rejection rates was provided after each block. Two training blocks were run prior to  
26  
27 161 the first experimental block.  
28

29  
30 162

31  
32 163 -----  
33

34 164 Insert Figure 1 about here  
35

36  
37 165 -----  
38

39  
40 166

### 41 42 167 **Processing of EEG data**

43  
44 168 EEG data, sampled at 500 Hz using a BrainVision amplifier, were DC-recorded  
45  
46 169 from 64 Ag/AgCl active electrodes at standard locations of the extended 10-20  
47  
48 170 system. Two electrodes at the outer canthi of the eyes monitored lateral eye  
49  
50 171 movements (horizontal electrooculogram, HEOG) and electrodes sites TP9/10 were  
51  
52 172 used as mastoid references. Continuous EEG data was referenced to the left mastoid  
53  
54 173 during recording, and was offline re-referenced to the arithmetic mean of both  
55  
56 174 mastoids and submitted to a 40Hz low-pass finite impulse response filter (Blackman  
57  
58  
59  
60

1  
2  
3 175 window, filter order 666). EEG epochs for the 2000 ms interval following sample  
4  
5 176 stimulus onset were computed relative to a 200 ms pre-stimulus baseline. Blind  
6  
7 177 source separation of EEG data was performed with the Independent Component  
8  
9 178 Analysis (ICA) algorithm implemented in the EEGLab toolbox (Delorme and Makeig  
10  
11 179 2004; Delorme, Sejnowski, Makeig 2007). Independent components related to  
12  
13 180 artifacts at anterior scalp regions (in particular, eye movements and blinks), were  
14  
15 181 identified by visual inspection and subtracted from the EEG data. To obtain reliable  
16  
17 182 ICA decompositions, a copy of the data was segmented into eight 250 ms frames  
18  
19 183 covering the 2000 ms retention period. These frames were corrected using whole-  
20  
21 184 epoch baselines to achieve data stationarity (cf., Groppe, Makeig, Kutas 2009)  
22  
23 185 without high-pass filtering, which would have removed slow brain potentials. The  
24  
25 186 copy was discarded after ICA decompositions had been applied to the original data  
26  
27 187 set. Epochs with lateral eye movements that escaped ICA artifact correction were  
28  
29 188 identified and removed with a differential step function on the bipolarized HEOG (step  
30  
31 189 width 100 ms, threshold 24  $\mu$ V). The resulting HEOG waveforms contained no  
32  
33 190 systematic eye gaze deflections towards the task-relevant hand (Figure 2, bottom  
34  
35 191 panel). After artifact rejection and elimination of trials with incorrect responses, 90.2%  
36  
37 192 of all epochs were retained for statistical analyses (low load: 93.4%; high load:  
38  
39 193 87.1%).  
40  
41  
42  
43  
44  
45  
46

194

## 195 **Results**

### 196 **Behavioral performance**

197 Participants responded correctly on 97.1% of all low-load trials and 90.4% of  
198 all high-load trials. Sensitivity indices ( $d'$ ) were analysed in a two-way repeated  
199 measures ANOVA with the factors memory load (low, high) and relevant hand (left,  
200 right). Performance was reduced with high load relative to low load ( $F(1,15) = 71.728$ ,

200

201

202

203

204

1  
2  
3 201  $p < 10^{-6}$ ), and did not differ between blocks where the left or right hand was relevant  
4  
5 202 ( $F(1,15) = 1.081, p > 0.3$ ). A significant memory load x relevant hand interaction  
6  
7 203 ( $F(1,15) = 6.222, p = 0.025$ ) was due to the fact that the performance decrement with  
8  
9 204 high as compared to low memory load was larger when the memory task was  
10  
11 205 performed with the left hand (8.5%) relative to blocks where the right hand was  
12  
13 206 relevant (4.9%).

16 207 Mean vocal reaction times (RTs) in trials with correct responses were faster in  
17  
18 208 the low-load relative to the high-load condition (799 ms versus 817 ms; main effect of  
19  
20 209 memory load:  $F(1,15) = 8.801, p = 0.010$ ). RTs did not differ between blocks where  
21  
22 210 the left or right hand was task-relevant ( $F(1, 15) = 1.846, p > 0.1$ ). The memory load x  
23  
24 211 relevant hand interaction was significant ( $F(1,15) = 5.25, p = 0.037$ ), as the RT costs  
25  
26 212 for the low-load versus high-load condition were larger when the memory task was  
27  
28 213 performed with the right hand (26 ms) relative to blocks where the left hand was  
29  
30 214 relevant (10 ms). In other words, there was an asymmetric speed-accuracy tradeoff  
31  
32 215 between the two hands for task performance in the high-load versus low-load  
33  
34 216 condition.

37  
38  
39 217

### 41 218 **Electrophysiological data**

42  
43 219 Figure 2 shows ERP waveforms averaged across lateral central electrodes (FC3/4,  
44  
45 220 FC5/6, C3/4, C5/6, CP3/4, CP5/6) contralateral and ipsilateral to the task-relevant  
46  
47 221 hand for the 2000 ms interval between the bilateral sample stimulus and the  
48  
49 222 subsequent test stimulus. Results are shown separately for the low-load and high-  
50  
51 223 load conditions. Following the early sensory-evoked ERP components to the sample  
52  
53 224 stimulus, ERP waveforms were characterized by a gradually developing sustained  
54  
55 225 negativity that reached its maximal amplitude immediately before the onset of the test  
56  
57  
58  
59  
60

1  
2  
3 226 stimuli. This sustained negativity that was present at contralateral as well as  
4  
5 227 ipsilateral electrodes reflects the Contingent Negative Variation (CNV; see Birbaumer  
6  
7 228 et al. 1990) that is elicited in anticipation of expected task-relevant events such as the  
8  
9  
10 229 test stimulus set used in this study. More importantly, sample stimuli triggered a  
11  
12 230 transient enhanced negativity contralateral to the task-relevant hand. This N2cc  
13  
14 231 component emerged around 180 ms after sample stimulus onset, and its amplitude  
15  
16 232 was larger in the high-load as compared to the low-load condition. The N2cc was  
17  
18 233 followed by a sustained contralateral negativity (tCDA) that remained present  
19  
20 234 throughout the retention period. This tCDA component was larger when two tactile  
21  
22 235 stimuli had to be memorized relative to the low load condition. The topographical  
23  
24 236 maps in Figure 2 illustrate the scalp distribution of N2cc and tCDA components in the  
25  
26 237 low-load and high-load conditions. Data shown in these maps were collapsed across  
27  
28 238 blocks where the left or right hand was task-relevant by flipping ERPs at contralateral  
29  
30 239 electrodes in blocks with a left-hand memory task over the midline. Both N2cc and  
31  
32 240 tCDA components were maximal over somatosensory areas in the postcentral gyrus  
33  
34 241 and adjacent parietal regions (see also Figure 4 below).

242

243 -----

244 Insert Figure 2 about here

245 -----

246

247 Difference waveforms were computed by subtracting ERPs ipsilateral to the  
248 currently task-relevant hand from contralateral ERPs. Statistical tests were conducted  
249 on mean amplitudes of these difference waves for a time window centered on the  
250 N2cc component (180-260 ms post-stimulus), and a second window centered on the

1  
2  
3 251 tCDA (300-2000 ms). Difference values that statistically differ from zero mark the  
4  
5 252 presence of reliable lateralized components in the ERP waveforms. The N2cc was  
6  
7 253 present in both the low-load ( $t(15) = -5.593, p < 10^{-4}$ ) and high-load condition ( $t(15) =$   
8  
9  
10 254  $-7.037, p < 10^{-5}$ ). N2cc amplitudes were significantly larger with high relative to low  
11  
12 255 memory load ( $t(15) = 4.235, p < 10^{-3}$ ). The tCDA component was present with low  
13  
14 256 load ( $t(15) = -2.951, p = 0.010$ ) as well as with high memory load ( $t(15) = -6.126, p <$   
15  
16 257  $10^{-4}$ ). Similar to the N2cc, tCDA amplitudes were significantly larger in the high-load  
17  
18 258 relative to the low-load condition ( $t(15) = 3.801, p = 0.002$ ).

20  
21 259 An additional analysis of mean amplitudes in the tCDA time window obtained  
22  
23 260 for the unsubtracted ERP waveforms revealed a main effect of contralaterality  
24  
25 261 (electrodes contralateral versus ipsilateral to the task-relevant hand;  $F(1,15) =$   
26  
27 262  $38.006, p < 10^{-4}$ ) that interacted with load ( $F(1,15) = 14.448, p = 0.002$ ), due to the  
28  
29 263 fact that the tCDA was larger in the high-load condition. There was also a main effect  
30  
31 264 of load ( $F(1,15) = 14.862, p=0.002$ ), with larger CNV components with high memory  
32  
33 265 load. This load-dependent modulation of CNV amplitudes was reliable at contralateral  
34  
35 266 as well as ipsilateral electrodes  $t(15) = -4.500$  and  $-2.481, p < 0.001$  and  $0.026,$   
36  
37 267 respectively).

40  
41 268 Tactile working memory capacity was calculated for each individual participant  
42  
43 269 on the basis of their performance in the high-load condition, using the formula  $K =$   
44  
45 270  $(hits + correct\ rejections - 1) \times 2$ , where 2 denotes memory set size in this condition  
46  
47 271 (Cowan 2001). As illustrated in Figure 3, individual memory capacity was reliably  
48  
49 272 correlated with the difference of tCDA amplitudes between the high-load and low-load  
50  
51 273 conditions ( $r = -0.640, p = 0.008$ ). Participants with higher tactile working memory  
52  
53 274 capacity showed a more pronounced increase of the tCDA component on trials with  
54  
55 275 high versus low memory load than participants with lower capacity. No correlation  
56  
57  
58  
59  
60

1  
2  
3 276 was found between individual K values and the difference of N2cc amplitudes  
4  
5 277 between high- and low-load conditions ( $p > 0.7$ ).  
6

7 278 To obtain additional evidence for a link between tCDA amplitudes and  
8  
9 279 behavioral performance at the level of individual trials in the high-load condition, we  
10  
11 280 computed tCDA components in the high-load condition separately for trials with vocal  
12  
13 281 RTs above and below the median RT (with RT median splits conducted individually  
14  
15 282 for each participant and trial condition). Trials with fast responses were more  
16  
17 283 accurate than slow response trials (Cowan's K: fast = 1.786, slow = 1.453;  $t(15) =$   
18  
19 284 6.362,  $p < 10^{-4}$ ). Critically, tCDA amplitudes were larger for fast as compared to slow  
20  
21 285 response trials (-0.749  $\mu\text{V}$  versus -0.594  $\mu\text{V}$ ), and this amplitude difference was  
22  
23 286 significant ( $t(15) = -2.564$ ,  $p = 0.022$ ).  
24  
25  
26  
27

28 287

29 288 -----

30  
31  
32 289 Insert Figure 3 about here  
33  
34

35 290 -----

36  
37 291

38  
39  
40 292 An additional current source density (CSD) analysis was conducted to further  
41  
42 293 illustrate the modality-specific scalp topographies of the N2cc and tCDA components,  
43  
44 294 and to demonstrate that the selection of lateral central electrodes for the analysis of  
45  
46 295 these components was appropriate. ERP data were collapsed across the low- and  
47  
48 296 high-load conditions, after conversion of scalp potentials to surface Laplacians  
49  
50 297 ( $\lambda = 10^{-5}$ , iterations = 50,  $m = 4$ ; cf. Tenke and Kayser 2012). This  
51  
52 298 transformation minimizes effects of volume conduction from remote sources, and  
53  
54 299 leads to a reference-independent representation of EEG/ERP data. CSD  
55  
56 300 topographies provide a conservative estimate of the neural generator patterns that  
57  
58  
59  
60

1  
2  
3 301 contribute to scalp-recorded ERPs (Nunez and Westdorp 1994; Tenke and Kayser  
4  
5 302 2012). Robust lateralized effects were found over somatosensory brain regions  
6  
7 303 (Figure 4), as demonstrated by significant differences of contra- minus ipsilateral  
8  
9 304 activity recorded at central electrodes in the time window of N2cc ( $t(15) = -6.476$ ,  $p <$   
10  
11 305  $10^{-4}$ ) and tCDA ( $t(15) = -4.066$ ,  $p = 0.001$ ). Apart from an almost significant  
12  
13 306 contralateral positivity at anterior regions during the N2cc time window ( $t(15) = 2.107$ ,  
14  
15 307  $p = 0.052$ ), no statistically reliable lateralization was evident over posterior  
16  
17 308 (electrodes P3/4, P5/6, PO3/4, PO7/8) and anterior (electrodes AF3/4, AF7/8, F3/4,  
18  
19 309 F5/6) scalp regions (all  $p$ s  $> 0.2$ ; see Figure 4).  
20  
21  
22  
23  
24  
25  
26  
27  
28  
29  
30  
31  
32  
33  
34  
35  
36  
37  
38  
39  
40

310  
311 -----  
312 Insert Figure 4 about here  
313 -----  
314  
315

## 316 Discussion

317 We employed a tactile memory task that was modelled on the delayed match-  
318 to-sample task used in previous research on visual working memory (e.g., Vogel and  
319 Machizawa 2004) to identify ERP correlates of the selection and maintenance of  
320 task-relevant tactile stimuli. When participants memorized the spatial locations of one  
321 or two tactile sample pulses on the left or the right hand, an enhanced negativity with  
322 a centroparietal focus emerged contralateral to the hand where the memorized tactile  
323 sample was delivered. This tCDA component was sensitive to tactile working memory  
324 load, as it was larger on trials where participants had to remember two tactile  
325 stimulus locations than when only a single tactile location had to be memorized  
60

1  
2  
3 326 (Figure 2). The load-dependent increase of tCDA amplitudes was more pronounced  
4  
5 327 for participants with higher tactile working memory capacity than for individuals  
6  
7 328 whose capacity (measured by Cowan's K) was closer to 1 (Figure 3), mirroring  
8  
9  
10 329 previous findings for the visual CDA component (Vogel and Machizawa 2004).  
11  
12 330 Furthermore, the tCDA component was reliably larger on trials with fast vocal  
13  
14 331 responses in the high-load condition, which were also more accurate than slow  
15  
16 332 responses. This demonstrates that the tCDA component is linked to behavioral  
17  
18 333 performance on individual trials. These observations strongly suggest that the tCDA  
19  
20 334 is an electrophysiological correlate of the maintenance of somatosensory information  
21  
22 335 in tactile working memory.

23  
24  
25 336 Analogous to the visual CDA, which has a modality-specific topography over  
26  
27 337 posterior visual cortex (McCollough, Machizawa, Vogel 2007), the tactile CDA  
28  
29 338 component emerged at contralateral central electrodes. The scalp topography of the  
30  
31 339 tCDA in a CSD-transformed map (Figure 4) also suggests neural generators that are  
32  
33 340 located within the somatosensory system. We conclude that the tCDA component  
34  
35 341 reflects the spatially selective activation of modality-specific brain regions  
36  
37 342 contralateral to the task-relevant hand during the retention of tactile stimuli in working  
38  
39 343 memory. These results provide new support for the sensory recruitment model, which  
40  
41 344 assumes that brain regions involved in the perceptual processing of sensory stimuli  
42  
43 345 are also active during the maintenance of these stimuli in working memory. It should  
44  
45 346 be noted that topographical distributions of CSD-transformed scalp maps only allow  
46  
47 347 relatively coarse approximations of the neural origins of components such as the  
48  
49 348 tCDA, and that the exact anatomical basis of this component needs to be determined  
50  
51 349 in future work.

52  
53  
54  
55  
56  
57 350 Previous research has used transcranial magnetic stimulation (TMS; Harris et  
58  
59 351 al. 2002) and EEG source reconstruction techniques in studies with human  
60



1  
2  
3 352 participants (Spitzer and Blankenburg 2011), as well as single-cell recordings in  
4  
5 353 monkeys (Romo and Salinas 2003) to show that the activity of neurons in primary  
6  
7 354 (SI) and secondary (SII) somatosensory cortex is modulated in tactile working  
8  
9 355 memory tasks. For example, a suppression of alpha activity indicative of attentional  
10  
11 356 processing was found over contralateral SI during the retention period of a  
12  
13 357 vibrotactile frequency discrimination task (Spitzer and Blankenburg 2011).  
14  
15 358 Asymmetric alpha band oscillations have also been suggested as the physiological  
16  
17 359 basis of the visual CDA component (van Dijk et al. 2010). Indirect evidence for a  
18  
19 360 recruitment of somatosensory brain areas comes from a tactile EEG study that used  
20  
21 361 task-irrelevant probe stimuli presented during the retention period to examine how  
22  
23 362 working memory influences somatosensory encoding (Katus, Andersen, Müller  
24  
25 363 2012). The retention of locations in working memory was mirrored by spatially  
26  
27 364 selective modulation of early ERP components to tactile probe stimuli with putative  
28  
29 365 origins in somatosensory areas such as SII (Frot and Mauguière 1999). These lines  
30  
31 366 of evidence point towards close links between the maintenance of tactile information  
32  
33 367 in working memory and the spatially specific activation of early somatosensory areas.  
34  
35 368 The critical new finding of the present study is the discovery of the tCDA component  
36  
37 369 that reflects the maintenance of tactile information in a sustained and load-dependent  
38  
39 370 manner. Because the tCDA is computed by comparing ERPs at electrodes  
40  
41 371 contralateral and ipsilateral to the location of memorized tactile events, it only reflects  
42  
43 372 the difference in the absolute activation of contralateral versus ipsilateral  
44  
45 373 somatosensory areas, and should therefore not be interpreted as evidence that  
46  
47 374 tactile working memory storage is exclusively contralateral. In fact, there is  
48  
49 375 electrophysiological evidence that ipsilateral somatosensory cortex may also be  
50  
51 376 involved in the maintenance of tactile pattern information (Li Hegner et al. 2007).  
52  
53  
54  
55  
56  
57  
58  
59  
60

1  
2  
3 377 The tCDA component was preceded by an earlier contralateral negativity,  
4  
5 378 (N2cc component) which emerged around 180 ms after sample stimulus onset.  
6  
7 379 Similar to the tCDA, the N2cc showed a centroparietal scalp topography (see Figures  
8  
9  
10 380 2 and 4), and was larger in the high-load as compared to the low-load condition. This  
11  
12 381 new N2cc component is likely to represent the somatosensory equivalent of the well-  
13  
14 382 known visual N2pc component. The N2pc is triggered at contralateral posterior  
15  
16 383 electrodes at a similar post-stimulus latency during the attentional selection of targets  
17  
18 384 among distractors in visual displays (Eimer 1996; Luck and Hillyard 1994), and  
19  
20 385 precedes the CDA in visual working memory studies that employ a similar delayed  
21  
22 386 match-to-sample task as the one used in the present study (e.g., Anderson, Vogel,  
23  
24 387 Awh 2011; McCollough, Machizawa, Vogel 2007). The load-dependent increase of  
25  
26 388 the tactile N2cc component observed in the present study mirrors previous findings  
27  
28 389 for the visual N2pc, which increases in size with the number of attended objects in  
29  
30 390 visual displays (e.g., Drew and Vogel 2008; Mazza and Caramazza 2011).

31  
32  
33  
34 391 The absence of N2cc components in previous ERP studies of tactile spatial  
35  
36 392 attention is due to the fact that instead of employing bilateral stimuli, tactile events  
37  
38 393 were delivered to a single location on the left or right hand. In these studies, modality-  
39  
40 394 specific components of the somatosensory event-related potential, such as the P100  
41  
42 395 or N140, were found to be larger for tactile stimuli at currently attended as compared  
43  
44 396 to unattended positions (e.g., Forster and Eimer 2005), demonstrating that spatial  
45  
46 397 attention enhances the sensory processing of tactile events. Analogous to the visual  
47  
48 398 N2pc, which is elicited when target and distractor objects appear in both visual  
49  
50 399 hemifields, measurement of the N2cc component requires that relevant and irrelevant  
51  
52 400 tactile events are presented simultaneously to both hands, or to other homologous  
53  
54 401 locations on the left and right side of the body. Note that the modality-specific  
55  
56 402 somatosensory N2cc component found here is distinct from another ERP component  
57  
58  
59  
60

1  
2  
3 403 with the same label that has been observed in stimulus-response compatibility  
4  
5 404 experiments, and is linked to visuospatially guided response selection (Praamstra  
6  
7 405 and Oostenveld 2003). The question whether the effects of memory load on the N2cc  
8  
9  
10 406 and tCDA components reflect load-sensitive modulations of two distinct processing  
11  
12 407 stages (i.e., the attentional selection and the subsequent storage of task-relevant  
13  
14 408 tactile information in working memory), or of a single memory maintenance stage that  
15  
16 409 temporally overlaps with the N2cc component needs to be investigated in future  
17  
18 410 studies where the demands on attentional target selection and working memory load  
19  
20 411 are independently manipulated. In addition to the N2cc and tCDA components, a  
21  
22 412 sustained bilateral CNV component that was observed in the interval between  
23  
24 413 sample and test stimuli was also modulated by memory load. This modulation may  
25  
26 414 primarily reflect differences in the preparation for the match/mismatch decision in  
27  
28 415 response to the test stimulus, which is more demanding in the high-load condition.  
29  
30 416 However, the presence of load effects at ipsilateral electrodes could in principle as  
31  
32 417 well reflect contributions of ipsilateral somatosensory cortex to working memory  
33  
34 418 maintenance (Li Hegner et al. 2007; see also van Ede, Lange, Maris 2013).

35  
36  
37  
38  
39 419 When considered together with the results of previous ERP investigations of  
40  
41 420 visual working memory (Anderson, Vogel, Awh 2011; McCollough, Machizawa, Vogel  
42  
43 421 2007; Vogel, McCollough, Machizawa 2005; Vogel and Machizawa 2004), the current  
44  
45 422 findings reveal striking similarities between the mechanisms that underlie the spatial  
46  
47 423 selection and selective maintenance of sensory stimuli in vision and touch. During  
48  
49 424 both visual and tactile working memory tasks, two contralateral ERP components are  
50  
51 425 elicited successively, with a highly similar time course in both modalities. N2pc and  
52  
53 426 N2cc components that emerge around 180 ms after sample display onset reflect  
54  
55 427 spatial selection during encoding of task-relevant visual or tactile information. The  
56  
57 428 subsequent CDA and tCDA components are linked to the sustained maintenance of  
58  
59  
60

1  
2  
3 429 stored information during the retention period. The fact that the load-sensitive tCDA  
4  
5 430 component observed in this study showed a topography over lateral central  
6  
7 431 somatosensory areas (see Figure 4), while the visual CDA component is elicited over  
8  
9 432 lateral posterior visual cortex (McCollough, Machizawa, Vogel 2007) strongly  
10  
11 433 suggests that the maintenance of visual or tactile information in working memory  
12  
13 434 involves the activation of distinct modality-specific regions, in line with the sensory  
14  
15 435 recruitment model of working memory (D'Esposito 2007; Pasternak and Greenlee  
16  
17 436 2005; Postle 2006; Sreenivasan, Curtis, D'Esposito 2014). In both vision and touch,  
18  
19 437 neural networks that mediate the perceptual processing of sensory signals contribute  
20  
21 438 to the storage and maintenance of information in working memory.  
22  
23  
24  
25  
26  
27

#### 28 **Acknowledgments**

29  
30 441 This work was funded by the Deutsche Forschungsgemeinschaft (DFG grant KA  
31  
32 442 3843/1-1). We thank Sue Nicholas for invaluable help in setting up the hardware  
33  
34 443 used for tactile stimulation.  
35  
36  
37  
38  
39

#### 40 **References**

41  
42 446 Anderson DE, Vogel EK, Awh E. 2011. Precision in visual working memory reaches a  
43  
44 447 stable plateau when individual item limits are exceeded. *J Neurosci.* 31(3):1128–  
45  
46 448 1138.  
47  
48 449 Birbaumer N, Elbert T, Canavan AG, Rockstroh, B 1990. Slow potentials of the  
49  
50 450 cerebral cortex and behavior. *Physiol Rev.* 70(1): 1-41.  
51  
52 451 Cowan N. 2001. The magical number 4 in short-term memory: a reconsideration of  
53  
54 452 mental storage capacity. *Behav Brain Sci.* 24(1):87-114x.  
55  
56  
57  
58  
59  
60

- 1  
2  
3 453 Curtis CE, D'Esposito M. 2003. Persistent activity in the prefrontal cortex during  
4  
5 454 working memory. *Trends Cogn Sci.* 7(9):415–423.  
6  
7 455 Curtis CE, Rao VY, D'Esposito M. 2004. Maintenance of spatial and motor codes  
8  
9 456 during oculomotor delayed response tasks. *J Neurosci.* 24(16):3944–3952.  
10  
11 457 Delorme A, Makeig S. 2004. EEGLAB: an open source toolbox for analysis of single-  
12  
13 458 trial EEG dynamics including independent component analysis. *J Neurosci*  
14  
15 459 *Methods.* 134(1):9–21.  
16  
17 460 Delorme A, Sejnowski T, Makeig S. 2007. Enhanced detection of artifacts in EEG  
18  
19 461 data using higher-order statistics and independent component analysis.  
20  
21 462 *Neuroimage.* 34(4):1443–1449.  
22  
23 463 D'Esposito M. 2007. From cognitive to neural models of working memory. *Philos*  
24  
25 464 *Trans R Soc Lond B Biol Sci.* 362(1481):761–772.  
26  
27 465 Drew T, Vogel EK. 2008. Neural measures of individual differences in selecting and  
28  
29 466 tracking multiple moving objects. *J Neurosci.* 28(16):4183–4191.  
30  
31 467 Eimer M. 1996. The N2pc component as an indicator of attentional selectivity.  
32  
33 468 *Electroencephalogr Clin Neurophysiol.* 99(3):225–234.  
34  
35 469 Forster B, Eimer M. 2005. Covert attention in touch: Behavioral and ERP evidence  
36  
37 470 for costs and benefits. *Psychophysiology.* 42(2):171–179.  
38  
39 471 Frot M, Mauguière F. 1999. Timing and spatial distribution of somatosensory  
40  
41 472 responses recorded in the upper bank of the sylvian fissure (SII area) in humans.  
42  
43 473 *Cereb Cortex.* 9(8):854–863.  
44  
45 474 Fuster JM, Alexander GE. 1971. Neuron activity related to short-term memory.  
46  
47 475 *Science.* 173(3997):652–654.  
48  
49 476 Groppe DM, Makeig S, Kutas M. 2009. Identifying reliable independent components  
50  
51 477 via split-half comparisons. *Neuroimage.* 45(4):1199–1211.  
52  
53  
54  
55  
56  
57  
58  
59  
60

- 1  
2  
3 478 Harris JA, Miniussi C, Harris IM, Diamond ME. 2002. Transient storage of a tactile  
4  
5 479 memory trace in primary somatosensory cortex. *J Neurosci.* 22(19):8720–8725.  
6  
7 480 Harrison SA, Tong F. 2009. Decoding reveals the contents of visual working memory  
8  
9 481 in early visual areas. *Nature.* 458(7238):632–635.  
10  
11 482 Kaas AL, van Mier H, Visser M, Goebel R. 2013. The neural substrate for working  
12  
13 483 memory of tactile surface texture. *Hum Brain Mapp.* 34(5):1148–1162.  
14  
15 484 Katus T, Andersen SK, Müller MM. 2012. Maintenance of tactile short-term memory  
16  
17 485 for locations is mediated by spatial attention. *Biol Psychol.* 89(1):39–46.  
18  
19 486 Kostopoulos P, Albanese M, Petrides M. 2007. Ventrolateral prefrontal cortex and  
20  
21 487 tactile memory disambiguation in the human brain. *Proc Natl Acad Sci USA.*  
22  
23 488 104(24):10223–10228.  
24  
25 489 Lee SH, Kravitz DJ, Baker CI. 2013. Goal-dependent dissociation of visual and  
26  
27 490 prefrontal cortices during working memory. *Nature Neurosci.* 16(8), 997-999.  
28  
29 491 Li Hegner Y, Lutzenberger W, Leiberg S, Braun C. 2007. The involvement of  
30  
31 492 ipsilateral temporoparietal cortex in tactile pattern working memory as reflected in  
32  
33 493 beta event-related desynchronization. *Neuroimage.* 37(4): 1362–1370.  
34  
35 494 Lewis-Peacock JA, Drysdale AT, Oberauer K, Postle BR. 2012. Neural evidence for a  
36  
37 495 distinction between short-term memory and the focus of attention. *J Cogn*  
38  
39 496 *Neurosci.* 24(1): 61–79.  
40  
41 497 Luck SJ, Hillyard SA. 1994. Spatial filtering during visual search: Evidence from  
42  
43 498 human electrophysiology. *J Exp Psychol Hum Percept Perform.* 20(5):1000–1014.  
44  
45 499 Mazza V, Caramazza A. 2011. Temporal brain dynamics of multiple object  
46  
47 500 processing: the flexibility of individuation. *PLoS ONE.* 6(2):e17453.  
48  
49 501 McCollough AW, Machizawa MG, Vogel EK. 2007. Electrophysiological measures of  
50  
51 502 maintaining representations in visual working memory. *Cortex.* 43(1):77–94.  
52  
53  
54  
55  
56  
57  
58  
59  
60

- 1  
2  
3 503 Nunez PL, Westdorp AF. 1994. The surface Laplacian, high resolution EEG and  
4  
5 504 controversies. *Brain Topogr.* 6(3):221–226.  
6  
7 505 Pasternak T, Greenlee MW. 2005. Working memory in primate sensory systems. *Nat*  
8  
9 506 *Rev Neurosci.* 6(2):97–107.  
10  
11 507 Postle BR. 2005. Delay-period activity in the prefrontal cortex: one function is sensory  
12  
13 508 gating. *J Cogn Neurosci.* 17(11):1679–1690.  
14  
15 509 Postle BR. 2006. Working memory as an emergent property of the mind and brain.  
16  
17 510 *Neuroscience.* 139(1):23–38.  
18  
19 511 Postle BR, Awh E, Serences JT, Sutterer DW, D'Esposito M. 2013. The positional-  
20  
21 512 specificity effect reveals a passive-trace contribution to visual short-term memory.  
22  
23 513 *PLoS ONE.* 8(12): e83483.  
24  
25 514 Praamstra P, Oostenveld R. 2003. Attention and movement-related motor cortex  
26  
27 515 activation: a high-density EEG study of spatial stimulus-response compatibility.  
28  
29 516 *Brain Res Cogn Brain Res.* 16(3):309–322.  
30  
31 517 Romo R, Salinas E. 2003. Flutter discrimination: neural codes, perception, memory  
32  
33 518 and decision making. *Nat Rev Neurosci.* 4(3):203–218.  
34  
35 519 Spitzer B, Blankenburg F. 2011. Stimulus-dependent EEG activity reflects internal  
36  
37 520 updating of tactile working memory in humans. *Proc Natl Acad Sci USA.*  
38  
39 521 108(20):8444–8449.  
40  
41 522 Sreenivasan KK, Curtis CE, D'Esposito M. 2014. Revisiting the role of persistent  
42  
43 523 neural activity during working memory. *Trends Cogn Sci.* 18(2), 82-89.  
44  
45 524 Supèr H, Spekreijse H, Lamme VA. 2001. A neural correlate of working memory in  
46  
47 525 the monkey primary visual cortex. *Science.* 293(5527):120–124.  
48  
49 526 Tenke CE, Kayser J. 2012. Generator localization by current source density (CSD):  
50  
51 527 implications of volume conduction and field closure at intracranial and scalp  
52  
53 528 resolutions. *Clin Neurophysiol.* 123(12):2328–2345.  
54  
55  
56  
57  
58  
59  
60

- 1  
2  
3 529 van Dijk H, van der Werf J, Mazaheri A, Medendorp WP, Jensen O. 2010.  
4  
5 530 Modulations in oscillatory activity with amplitude asymmetry can produce  
6  
7 531 cognitively relevant event-related responses. *Proc Natl Acad Sci USA*. 107(2):  
8  
9 532 900–905.  
10  
11 533 van Ede F, de Lange FP, Maris E. 2013. Anticipation increases tactile stimulus  
12  
13 534 processing in the ipsilateral primary somatosensory cortex. *Cereb Cortex*.  
14  
15 535 Doi: 10.1093/cercor/bht111.  
16  
17 536 Vogel EK, McCollough AW, Machizawa MG. 2005. Neural measures reveal individual  
18  
19 537 differences in controlling access to working memory. *Nature*. 438(7067):500–503.  
20  
21 538 Zhou YD, Fuster JM. 1996. Mnemonic neuronal activity in somatosensory cortex.  
22  
23 539 *Proc Natl Acad Sci USA*. 93(19):10533–10537.  
24  
25  
26  
27  
28  
29  
30  
31  
32  
33

### 34 **Figure Legends**

35  
36 544 **Figure 1.** Illustration of the experimental setup. Participants memorized a tactile  
37  
38 545 sample set at one task-relevant hand to compare it with a test set on the same hand  
39  
40 546 after a 2 second retention period. Memory load was varied between trials (low load:  
41  
42 547 one pulse, high load: two pulses per hand). The relevant hand (left, right) was varied  
43  
44 548 between blocks. The example shown here illustrates a high-load trial where the  
45  
46 549 locations of tactile sample and test stimuli (symbolized by white dots) are identical at  
47  
48 550 the left hand (match), but not at the right hand (mismatch).  
49  
50  
51

52  
53  
54

55 552 **Figure 2.** Grand mean ERPs elicited in the 2000 ms interval following sample  
56  
57 553 stimulus onset in the low-load and high-load conditions. ERPs were averaged across  
58  
59  
60



1  
2  
3 554 lateral central electrode clusters contralateral (blue lines) and ipsilateral (red lines) to  
4  
5 555 the hand where the memory task was performed. Difference maps show the  
6  
7 556 topographical distribution of lateralized effects in the N2cc (bottom) and tCDA (top)  
8  
9  
10 557 time windows. These maps represent the amplitude difference of contralateral minus  
11  
12 558 ipsilateral recordings, collapsed across blocks where the memory task was  
13  
14 559 performed with the left or right hand. Enhanced contralateral negativities are shown  
15  
16 560 in blue. The two bottom panels show difference waveforms for the low-load and high-  
17  
18 561 load condition, obtained by subtracting electrodes ipsilateral to the task-relevant hand  
19  
20 562 from contralateral electrodes, and HEOG difference waveforms, calculated by  
21  
22 563 subtracting HEOG electrodes ipsilateral to the task-relevant hand from contralateral  
23  
24 564 electrodes after artifact rejection. In these HEOG difference waves, any eye  
25  
26 565 movements towards the task-relevant hand would be reflected by negative  
27  
28 566 (downward) HEOG deflections.  
29  
30  
31  
32  
33

34 568 **Figure 3.** Correlation of individual participant's tactile working memory capacity K (x-  
35  
36 569 axis) and the increase of tCDA amplitudes in the high-load relative to the low-load  
37  
38 570 condition measured for each participant (y-axis). K was calculated on the basis of  
39  
40 571 individual performance in the high-load condition.  
41  
42  
43  
44

45  
46 573 **Figure 4.** Grand mean current source density (CSD) topographical maps, showing  
47  
48 574 the scalp distribution of lateralized effects in the N2cc and tCDA time windows. These  
49  
50 575 maps represent the amplitude difference of contralateral minus ipsilateral recordings,  
51  
52 576 collapsed across blocks where the memory task was performed with the left or right  
53  
54 577 hand, and averaged across the low- and high-load conditions. Six electrodes at  
55  
56 578 lateral central scalp regions (black dots) were averaged for each recording cluster  
57  
58  
59  
60

1  
2  
3 579 (contra- and ipsilateral to the task-relevant hand). The presence of lateralized effects  
4  
5 580 was also tested for different sets of electrodes over anterior (white triangles) and  
6  
7 581 posterior (white crosses) scalp areas. Reliable lateralized effects were present only  
8  
9  
10 582 for the central electrode cluster.  
11  
12  
13  
14  
15  
16  
17  
18  
19  
20  
21  
22  
23  
24  
25  
26  
27  
28  
29  
30  
31  
32  
33  
34  
35  
36  
37  
38  
39  
40  
41  
42  
43  
44  
45  
46  
47  
48  
49  
50  
51  
52  
53  
54  
55  
56  
57  
58  
59  
60

For Peer Review

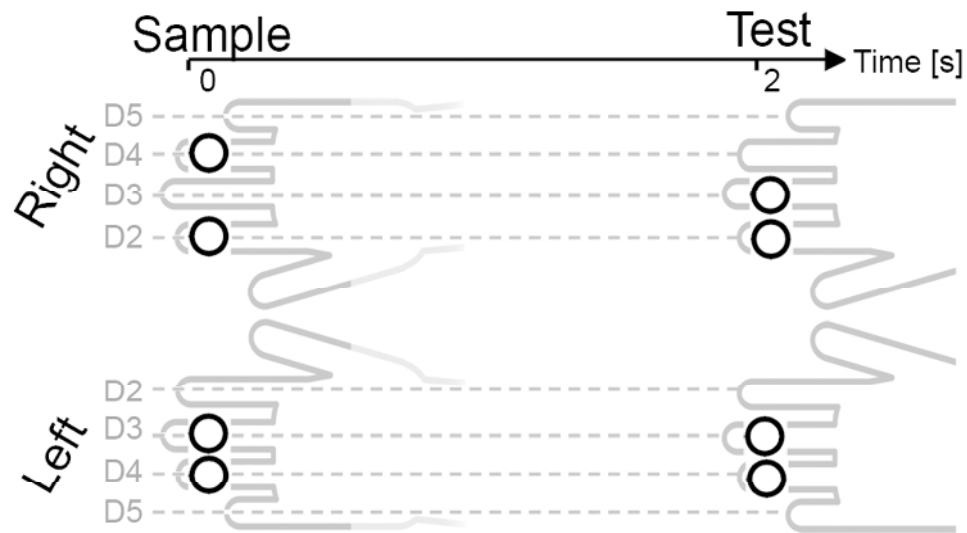


Figure 1. Illustration of the experimental setup. Participants memorized a tactile sample set at one task-relevant hand to compare it with a test set on the same hand after a 2 second retention period. Memory load was varied between trials (low load: one pulse, high load: two pulses per hand). The relevant hand (left, right) was varied between blocks. The example shown here illustrates a high-load trial where the locations of tactile sample and test stimuli (symbolized by white dots) are identical at the left hand (match), but not at the right hand (mismatch).

86x50mm (300 x 300 DPI)

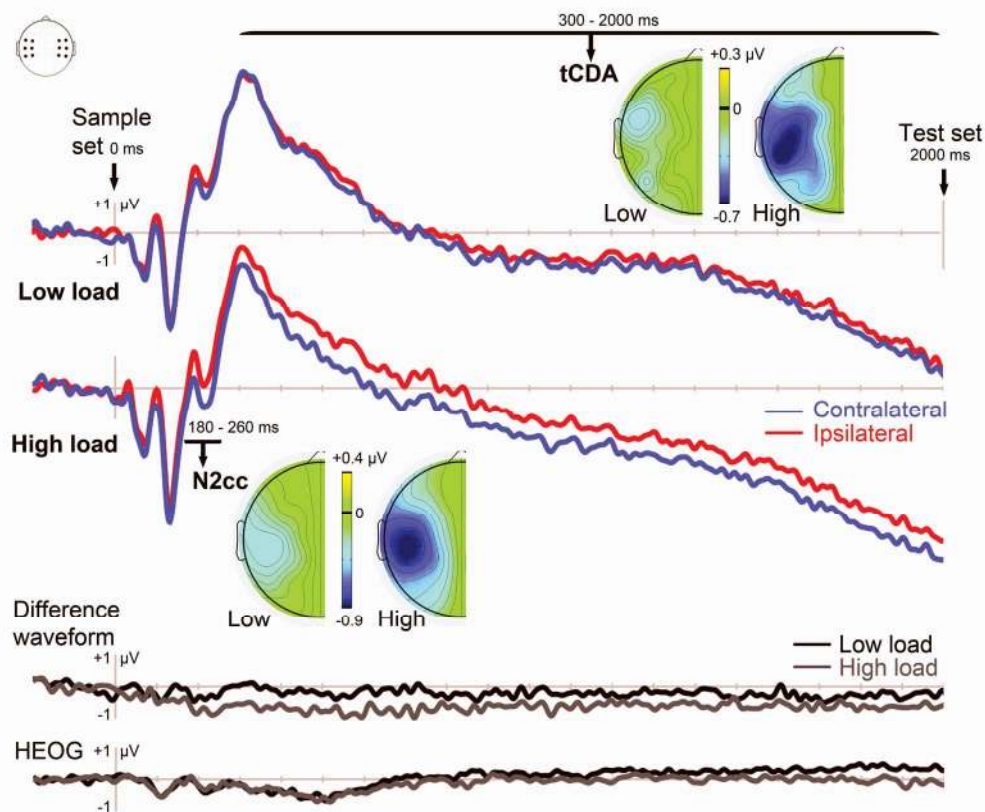


Figure 2. Grand mean ERPs elicited in the 2000 ms interval following sample stimulus onset in the low-load and high-load conditions. ERPs were averaged across lateral central electrode clusters contralateral (blue lines) and ipsilateral (red lines) to the hand where the memory task was performed. Difference maps show the topographical distribution of lateralized effects in the N2cc (bottom) and tCDA (top) time windows. These maps represent the amplitude difference of contralateral minus ipsilateral recordings, collapsed across blocks where the memory task was performed with the left or right hand. Enhanced contralateral negativities are shown in blue. The two bottom panels show difference waveforms for the low-load and high-load condition, obtained by subtracting electrodes ipsilateral to the task-relevant hand from contralateral electrodes, and HEOG difference waveforms, calculated by subtracting HEOG electrodes ipsilateral to the task-relevant hand from contralateral electrodes after artifact rejection. In these HEOG difference waves, any eye movements towards the task-relevant hand would be reflected by negative (downward) HEOG deflections.

180x148mm (300 x 300 DPI)

1  
2  
3  
4  
5  
6  
7  
8  
9  
10  
11  
12  
13  
14  
15  
16  
17  
18  
19  
20  
21  
22  
23  
24  
25  
26  
27  
28  
29  
30  
31  
32  
33  
34  
35  
36  
37  
38  
39  
40  
41  
42  
43  
44  
45  
46  
47  
48  
49  
50  
51  
52  
53  
54  
55  
56  
57  
58  
59  
60

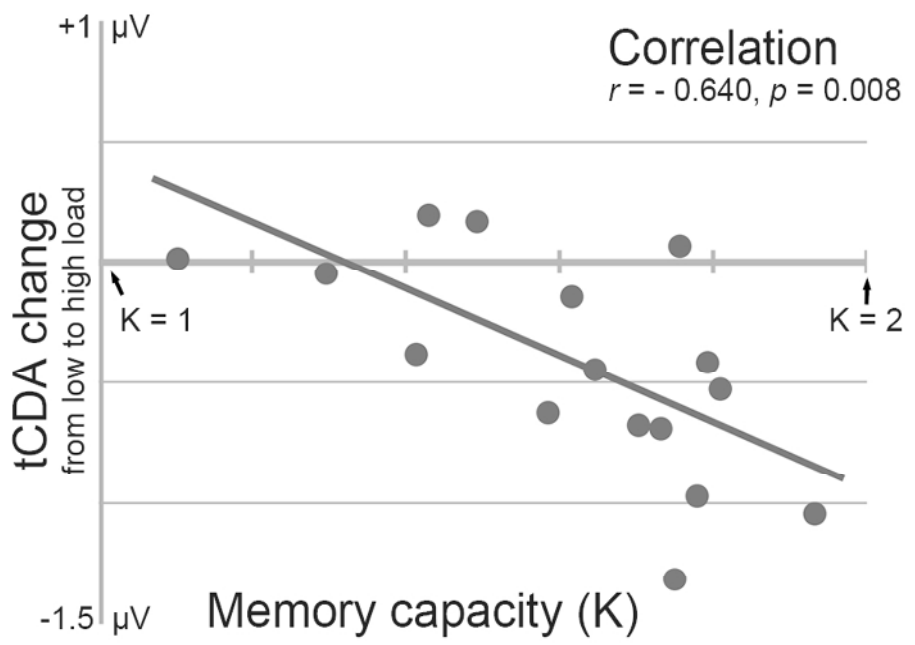


Figure 3. Correlation of individual participant's tactile working memory capacity K (x-axis) and the increase of tCDA amplitudes in the high-load relative to the low-load condition measured for each participant (y-axis). K was calculated on the basis of individual performance in the high-load condition. 86x61mm (300 x 300 DPI)

Review

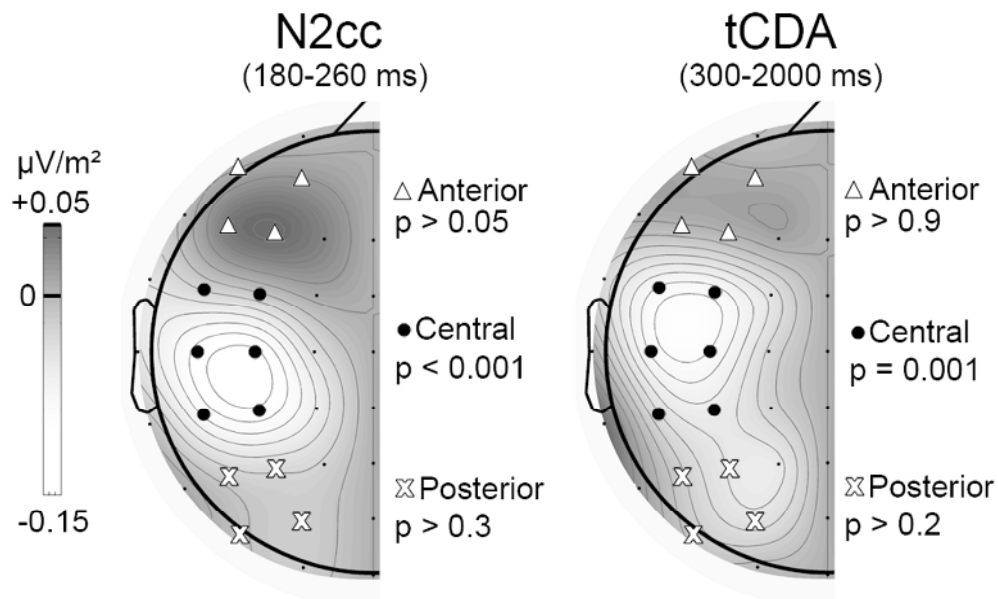


Figure 4. Grand mean current source density (CSD) topographical maps, showing the scalp distribution of lateralized effects in the N2cc and tCDA time windows. These maps represent the amplitude difference of contralateral minus ipsilateral recordings, collapsed across blocks where the memory task was performed with the left or right hand, and averaged across the low- and high-load conditions. Six electrodes at lateral central scalp regions (black dots) were averaged for each recording cluster (contra- and ipsilateral to the task-relevant hand). The presence of lateralized effects was also tested for different sets of electrodes over anterior (white triangles) and posterior (white crosses) scalp areas. Reliable lateralized effects were present only for the central electrode cluster.

86x52mm (300 x 300 DPI)